For COPD, regulation of miR-515-5p by hsa_circ_0061052, acting via the FoxC1/Snail pathway, is involved in cigarette smoke-induced airway remodeling

Qizhan Liu (drqzliu@hotmail.com)
Institute of Toxicology, School of Public Health, Nanjing Medical University

Huimin Ma
The Key Laboratory of Modern Toxicology,Ministry of Education, School of Public Health, Nanjing Medical University

Lu Lu
The Key Laboratory of Modern Toxicology, Ministry of Education, School of Public Health, Nanjing Medical University

Quanyong Xiang
Shanxi Center for Disease Control and Prevention

Haibo Xia
Institute of Microbiology Chinese Academy of Sciences

Jing Sun
The Key Laboratory of Modern Toxicology, Ministry of Education, School of Public Health, Nanjing Medical University

Junchao Xue
The Key Laboratory of Modern Toxicology, Ministry of Education, School of Public Health, Nanjing Medical University

Tian Xiao
The Key Laboratory of Modern Toxicology, Ministry of Education, School of Public Health, Nanjing Medical University

Cheng Cheng
The Key Laboratory of Modern Toxicology, Ministry of Education, School of Public Health, Nanjing Medical University

Aimin Shi
Jiangsu Animal Experimental Center for Medical and Pharmaceutical Research, Nanjing Medical University

Research

Keywords: CircRNA, Cigarette smoke, EMT, Airway remodeling, COPD

Posted Date: March 3rd, 2020

DOI: https://doi.org/10.21203/rs.3.rs-15783/v1

Abstract

Background

Regulatory networks involving non-coding RNA (ncRNA) are involved in various lung diseases. The function of circular RNA (circRNA), a recently recognized type of ncRNA, in chronic obstructive pulmonary disease (COPD), has not been elucidated.

Methods

Western blots and cellular immunofluorescence are used to check molecular biological changes and molecular interactions in cells, bioinformatics tools and luciferase reporter genes are used to assess molecular binding relationships, immunohistochemical examination of mouse lung tissue-related proteins A mouse model of COPD was used to validate related concubine mechanisms.

Results

In the present study, we aimed to determine whether hsa_circ_0061052 participates in the EMT of HBE cells and to elucidate its biological mechanism. Experiments with cultured cells and animals showed that exposure to cigarette smoke extract (CSE) or cigarette smoke (CS) induced the EMT and led to lung dysfunction and airway remodeling. For HBE cells and the lung tissues of CS-exposed mice, the expression of hsa_circ_0061052 was elevated. To verify the function of this circRNA, knocking it out in HBE cells reversed the CSE-induced EMT. We analyzed the regulatory relationship between hsa_circ_0061052 and miR-515-5p using bioinformatics, a luciferase reporter gene, and qRT-PCR. We found that hsa_circ_0061052 was mainly distributed in the cytoplasm and acted as a sponge for miR-515-5p. Assays with a luciferase reporter gene showed that miR-515-5p binds to the 3'UTR region of FoxC1 mRNA to inhibit its transcription. For HBE cells, overexpression of miR-515-5p reversed the CSE-induced EMT. In addition, hsa_circ_0061052 regulated the expression of FoxC1/Snail by competitively binding to miR-515-5p. When an hsa_circ_0061052 siRNA and an miR-515-5p inhibitor were co-transfected into HBE cells, the effect of hsa_circ_0061052 siRNA in reducing the EMT was reversed by the inhibitor; in animal models, this effect was also evident.

Conclusion

Experiments relating to the mechanisms of COPD airway remodeling due to the hsa_circ_0061052/miR-515-5p/FoxC1/Snail axis point to a biomarker for COPD and provide a basis for clinical application.

Background

Chronic obstructive pulmonary disease (COPD) is a public health problem. Because of its high prevalence, morbidity, and mortality, it poses a challenge to the healthcare system. Smoking is the primary risk factor for COPD [1, 2], but the molecular mechanism for this relationship is not clear. The main histological changes of COPD are epithelial remodeling and subepithelial fibrosis of small airways

[3, 4]. Remodeling of small airways leads to the airway dysfunction of COPD. A potential mechanism leading to airway remodeling is the epithelial-mesenchymal transition (EMT) [5, 6]. Components of cigarette smoke (CS), such as nicotine and benzopyrene, induce the EMT in immortalized cells from the airway epithelium [7-9]. As in our previous studies, exposure of human bronchial epithelial HBE cells to cigarette smoke extract (CSE) induced the EMT [10, 11]. Since current medications focus only on relieving symptoms and reducing the rate of deterioration [12], research on the molecular mechanism associated with COPD is needed.

Circular RNAs (circRNAs), which are non-coding RNAs, have a closed-loop structure and do not have a 5'cap or a 3' poly-A tail. RNase R, in the *E. coli* RNase superfamily, cuts and degrades RNA from the 3'-5 'direction. It digests almost all linear RNA molecules [13]. CircRNA is stably expressed and is not easily degraded by RNA exonucleases [14, 15]. As demonstrated with high-throughput sequencing, various human diseases have abnormal expression of circRNAs [16, 17]. Many circRNAs contain sites that allow them to bind to miRNAs competitively to reduce their inhibitory effects on target genes, and thereby to function in the regulation of gene expression [18]. For various lung diseases, there is abnormal expression of circRNAs [19-21]. Exposure of human small airway epithelial cells (HSAECs) to CSE causes changes in circRNAs, with hsa_circ_0061052 being the most up-regulated [22]. Thus, hsa_circ_0061052 may be related to the pathogenesis of COPD, but its molecular mechanism is not clear.

The human forkhead box (*Fox*) gene family has 19 subfamilies. These factors bind to the promoters of target genes or interact with other transcription factors to regulate a variety of biological processes in tissues and organs [23]. FoxC1, a member of the FOX transcription factor family [24], suppresses the transcription of E-cadherin (a biomarker of the EMT) by regulating the expression of Snail and thus induces the EMT [25]. Whether FoxC1 is involved in the CS-induced EMT remained to be explored.

We first measured the expression and function of hsa_circ_0061052, miR-515-5p, FoxC1, and Snail in CSE-treated HBE cells, focusing on the role of hsa_circ_0061052 in COPD, and on the hsa_circ_0061052 and miR-515-5p relationship in the CSE-induced EMT. The results elucidated a role of the hsa_circ_0061052/miR-515-5p/FoxC1 network in the CS-induced EMT, and led to a proposed molecular mechanism for the CS-induced EMT.

Methods

Preparation of CSE

CSE was prepared as previously reported [26]. Briefly, the smoke of a 3R4F Research Cigarette (University of Kentucky, USA) was bubbled into a flask containing 10 mL of warm (37 °C) RPMI-1640 medium by use of a vacuum pump at a constant speed (each cigarette was smoked for 5 min). The CSE solution was adjusted to pH 7.4 and then sterilized by filtration through a 0.22-μm pore filter (Schleicher & Schuell GmbH, Dassel, Germany). For quality control, the solution was standardized by monitoring the absorbance at 320 nm (A320) and 540 nm (A540). CSE quality was accepted if ΔOD (A320-A540) was

between 0.9 and 1.2. The resulting CSE solution, regarded as 100% CSE, was diluted with medium and used in experiments within 1 hour.

Cell culture and treatment

Simian virus 40 (SV40)-transformed human bronchial epithelial cells, which are nontumorigenic and retain features of parent HBE cells, were purchased from the Shanghai Institute of Cell Biology, Chinese Academy of Sciences (Shanghai, China). They were maintained in RPMI-1640 medium containing 10% fetal bovine serum (FBS, Life Technologies/Gibco, Grand Island, NY), 100 μg/mL streptomycin, and 100 U/mL penicillin (Life Technologies/Gibco, Gaithersburg, MD) under 5% CO_2 at 37°C. Cells were passaged at a ratio 1:3 every 2 days. After reaching 70-80% confluence, the cells were washed with phosphate-buffered saline, grown in RPMI-1640 medium supplemented with 10% FBS, and exposed to 0, 1, 2, or 4 % CSE for 48 hours.

RNA preparation and reverse-transcriptase polymerase chain reaction (RT-PCR)

The nuclear and cytoplasmic fractions of cells were extracted by use of the PARIS Kit Protein and RNA Isolation System (Thermo Fisher Scientific). Total RNA (1 μg) was treated with 10 U of RNase R (Epicentre Technologies Corp., Madison, WI) in 1× RNase R reaction buffer in a total volume of 10 μl. The mixture was incubated at 37 °C for 1 hour. Total RNA (1 μg) was transcribed into cDNA by HiScript II Q RT Supermix (Vazyme Biotech, Nanjing, China). The polymerase chain reaction reactions (PCR) were evaluated by checking the PCR products on 2% w/v agarose gels. The primers are listed in Table 1.

Table 1 Primer sequences used

hsa_circ_0061052	*5′-GGAGACAGGCATGGAGAAGA-3′*
	5′-GACCTGCACGGTCTCCTG-3′
GAPDH	*5′-GGAGCGAGATCCCTCCAAAAT-3′*
	5′- GGCTGTTGTCATACTTCTCATGG-3′
Mouse GAPDH	*5′-GTCTTCACTACCATGGAGAAGG-3′*
	5′-TCATGGATGACCTTGGCCAG-3′
miR-515-5p	*5′-GGGTTCTCCAAAAGAAAGCAC-3′*
	5′-CAGTGCGTGTCGTGGAGT-3′
miR-1182	*5′-GGGGAGGGTCTTGGGAGGGA-3′*
	5′-CAGTGCGTGTCGTGGAGT-3′
miR-1304-5p	*5′-GGGTTTGAGGCTACAGTGA-3′*
	5′-CAGTGCGTGTCGTGGAGT-3′

miR-136-5p *5′-GGGACTCCATTTGTTTTGAT-3′*

5′-CAGTGCGTGTCGTGGAGT-3′

U6 *5′-CGCTTCGGCAGCACATATACTAAAATTGGAAC-3′*

5′-GCTTCACGAATTTGCGTGTCATCCTTGC-3′

Quantitative real-time PCR

Total cellular RNA was isolated by Trizol (Invitrogen) according to the manufacturers' recommendations. To assess the circRNAs and the miRNAs, 1 mg of total RNA and HiScript II Q Select RT Supermix (Vazyme biotech) were used in reverse transcription according to the manufacturer's protocol. GAPDH RNA was used as a control. The primers are listed in Table 1. Quantitative real-time PCR was performed with Power SYBR Green Master Mix (Applied Biosystems, Foster City, CA, USA) and a LightCycler 96 instrument (Roche, Swiss). The fold change in the expression of each gene was calculated by the threshold cycle (Ct) method using the formula 2-(ΔΔCt)[27].

Western blots

Proteins extracted from cultured cells or lung tissues of mice (16 male BALB/c mice (age 6-8 weeks)) were quantified with BCA protein assay kits (Beyotime, China). Equal amounts (80 μg) of protein were separated by 10% SDS-PAGE and transferred to PVDF membranes (Millipore, USA). Membranes were then incubated overnight at 4 °C with a 1:1000 dilution of anti-glyceraldehyde 3-phosphate dehydrogenase (anti-GAPDH, Sigma) and an antibody for E-cadherin, N-cadherin, vimentin (Cell Signaling Technology, Beverly, MA), α-smooth muscle actin (α-SMA, Abcam), or FoxC1(Abcam). After additional incubation with a 1:1000 dilution of an anti-immunoglobin horseradish peroxidase-linked antibody for 1 h, the immune complexes were measured by enhanced chemiluminescence (Cell Signaling Technology). For densitometric analyses, protein bands on the blots were assessed by Image J software.

Fluorescence in situ hybridization assay (FISH)

FISH assays were performed with Fluorescence In situ Hybridization Kits (RiBoBio, Guangzhou, China). Briefly, cells grown on coverslips were fixed with 4% paraformaldehyde at room temperature for 10 min and treated with 0.5% Triton X-100 at 4 °C for 5 min. The samples were treated with pre-hybridization buffer at 37 °C for 30 min and then in hybridization buffer at 37 °C for 12–16 hours with a Cy3-labeled circRNA probe (Ribobio, Guangzhou, China) in a humid and dark environment. The samples were mounted with fluorescence mounting medium and imaged by use of a microscope (Zeiss, LSM700B, Germany).

Cell transfection

An miR-515-5p mimic, an miR-515-5p inhibitor, an miRNA negative control mimic (con mimic), an miRNA negative control inhibitor, hsa_circ_0061052 siRNA, and a control siRNA were synthesized by RiBoBio (Guangzhou, China). Cells were transiently transfected by use of Lipofectamine 2000 reagent (Invitrogen) according to the manufacturer's protocol. At 24 hours after transfection, cells were harvested and used for experiments.

Luciferase reporter assay

The binding of hsa_circ_0061052 to miR-515-5p and miR-515-5p to target genes was determined by luciferase-reporter assays. Either of two forms of hsa_circ_0061052 (wt-hsa_circ_0061052 or mut-hsa_circ_0061052) was cloned into a psiCHECK2 vector, and either of two forms of the FoxC1 3'-UTR (wt-FoxC1 3'-UTR or mut-FoxC1 3'-UTR) was cloned into a psiCHECK2 vector (Genechem Co., Ltd. Shanghai, China) and transfected into HBE cells. Luciferase activity was determined with Dual Luciferase Reporter Gene Assay Kits (Beyotime) according to the manufacturer's protocol. The Renilla luciferase activity was normalized by firefly luciferase.

Mice exposed to CS

Male BALB/c mice at 6-8 weeks of age were purchased from Animal Core Facility of Nanjing Medical University and housed in Jiangsu Province Medicine, Pesticide and Veterinary Drug Safety Evaluation and Research Center. Animals were treated humanely and with regard for alleviation of suffering according to a protocol approved by the Nanjing Medical University Animal Care and Use Committee.

To observe the effects of CS on airway obstruction of lungs, 16 male BALB/c mice (age 6-8 weeks) were divided into four groups: normal control and low-, medium-, and high-CS exposure groups. The low-, medium-, and high-CS groups were exposed in a whole-body exposure system (Beijing Huironghe Technology CO., Ltd., China) to CS from 3R4F Research Cigarettes (University of Kentucky, USA) at concentrations of 0, 100, 200, or 300 mg/m^3 total particulate matter (TPM) for 60 min twice a day, 4 hours apart, 5 days a week for a total of 16 weeks. Humidity, temperature, and O_2 level in the chamber were measured continuously during the exposure period. In the first week, there was increasing exposure, as follows: mice were placed in the chamber and exposed for 20 min on the first day, 30 min on the second day, and 60 min on the third day until the end. Age-matched mice kept in a similar environment without exposure to CS served as controls. Experiments were accomplished with n = 4 randomized animals per group.

Lung function measurement

For mice, airway hyper-responsiveness (AHR) was measured as the change in airway function by use of whole-body plethysmography (Buxco Electronics Ltd., USA), as previously reported [26]. Individual mice were placed unrestricted in a chamber connected to a pressure transducer to measure pressure changes inside the chamber. After acclimation, methacholine (0, 12.5, 25, or 50 mg/mL) were nebulized for 2 min, and enhanced pause (Penh) was recorded during the response period using FinePoint software (Buxco

Electronics Ltd., USA). Penh, a dimensionless unit, correlates with pulmonary resistance. Values were averaged and expressed as absolute Penh values.

Masson trichrome staining

The lungs of mice were fixed with 4% paraformaldehyde and embedded in paraffin. For histological analysis and detection of collagen deposition, successive 5-μm lung sections were placed on slides and subjected to staining with trichrome (Masson) kits (Sigma-Aldrich, Germany), according to the manufacturer's instructions. Collagen content was determined by the ratio of collagen surface area (blue) to total surface area (red). Image J software was used to evaluate collagen deposition.

Immunohistochemistry (IHC)

Mouse lungs were fixed with 4% paraformaldehyde and embedded in paraffin. To evaluate α-SMA expression, consecutive 5-μm lung sections were placed on glass slides and stained with an α-SMA stain according to the manufacturer's instructions (Solarbio Life Science, China). An IHC scoring (IRS) system was used to quantify IHC staining. The percentage of positively stained bronchial epithelial cells was as follows: 1 (<10%), 2 (10-50%), 3 (50-75%), and 4 (> 75%). Staining intensity was 0-3: 0, no staining; 1, weak staining (light yellow); 2, moderate staining (yellow-brown); 3, strong staining (brown). The staining index was obtained by multiplying the percentage of positive bronchial epithelial cells by the staining intensity, ranging from 0 to 12.

Statistical analyses

All experiments were performed in triplicate. Derived values are presented as means ± SD. Comparison of means among multiple groups was accomplished by one-way analysis of variance (ANOVA), and a multiple-range least significant difference (LSD) was used for inter-group comparisons. *P* values < 0.05 were considered statistically significant. All statistical analyses were performed with SPSS 18.0.

Results

CSE exposure induces the EMT and increases the levels of hsa_circ_0061052 in HBE cells

In organs, the EMT occurs during repair of chronic damage and in response to inflammation, such as fibrosis and COPD [28, 29]. HBE cells were exposed to 0, 1, 2, or 4% CSE for 48 hours. With the increased CSE exposure, levels of the epithelial marker protein, E-cadherin, decreased; there were elevated levels of the mesenchymal markers, N-cadherin, vimentin, and α-SMA (Fig. 1a and b). Immunofluorescence microscopy of E-cadherin and vimentin confirmed the location of EMT-related markers. The cells formed epithelial-like cell junctions and showed high levels of mesenchymal cell markers (Fig. 1c). After CSE treatment, hsa_circ_0061052 increased in a dose-response relationship (Fig. 1d and e). Thus these results show that, for HBE cells, CSE exposure induces the EMT and increases the levels of hsa_circ_0061052.

Characterization of hsa_circ_0061052 in HBE cells

Hsa_circ_0061052, derived from a host gene, oxysterol-binding protein 2 (*OSBPL2*), has a closed loop structure and a length of 253 nucleotides (Fig. 2a). Fluorescence in situ hybridization (FISH) revealed that hsa_circ_0061052 is located mainly in the cytoplasm of HBE cells (Fig. 2b). RT-PCR and qRT-PCR analysis of RNA in the nucleus and cytoplasm showed that hsa_circ_0061052 was concentrated in the cytoplasm (Fig. 2c and d). To verify the circular characteristics of hsa_circ_0061052, total RNA was processed with or without 10 U Rnase R for 1 hour. Hsa_circ_0061052 was resistant to exonucleases, but linear OSBPL2 mRNA was digested by exonucleases (Fig. 2e and f). These results show that hsa_circ_0061052 has a ring structure and is mainly concentrated in the cytoplasm.

Exposure of HBE cells to CSE decreases their levels of miR-515-5p and increases their levels of FoxC1/Snail, which is a target of miR-515-5p

CircRNA can act as a miRNA sponge and form a circRNA-miRNA regulatory network [30, 31]. Using the CircInteractome (http://circinteractome.nia.nih.gov/) database, we predicted the miRNAs that may be regulated by hsa_circ_0061052, and selected possible binding sites of hsa_circ_0061052 with miRNAs (Fig. 3a). The top five miRNAs (miR-515-5p, miR-1182, miR-1304, miR-136, and miR-571) were selected for analysis. QRT-PCR was performed after HBE cells were treated with 0, 1, 2, or 4% CSE for 48 hours. With increasing concentrations, CSE reduced the levels of miR-515-5p, but levels of miR-1182, miR-1304, miR-136, and miR-571 levels were not decreased (Fig. 3b). To verify the results, a luciferase reporter gene was constructed based on the complementary pairing binding site of hsa_circ_0061052 and miR-515-5p (Fig. 3c) and co-transfected into HBE cells with an miR-515-5p mimic or control (con) mimic. The relative luciferase activity was reduced in cells co-transfected with psiCHECK2-hsa_circ_0061052-wt and the miR-515-5p mimic (Fig. 3d). These results indicate that hsa_circ_0061052 can act as a miRNA sponge for miR-515-5p.

FoxC1, a member of the Fox family of transcription factors, increases Snail expression by activating the Snail promoter region, thereby inhibiting the transcription of E-cadherin and participating in the EMT [25]. HBE cells were exposed to 0, 1, 2, or 4% CSE for 48 hours. With the increase of CSE exposure, the levels of FoxC1 and Snail increased (Fig. 3e and f). We used the bioinformatics tools miRanda (http: // www.microrna.org/) and TargetScan (http://www.targrtscan.org/) to predict that FoxC1 is a target of miR-515-5p. Consistent with the binding site of miR-515-5p in the 3'UTR region of FoxC1 mRNA (Fig. 3g), a luciferase reporter gene was constructed and co-transfected with an miR-515-5p mimic or control. Co-transfection of the miR-515-5p mimic reduced the relative luciferase activity with the wt-FoxC1 3'UTR vector (Fig. 3h). These results show that, in HBE cells, FoxC1 is a target of miR-515-5p and that CSE increases the levels of FoxC1 and Snail.

In HBE cells, hsa_circ_0061052 is involved in the CSE-induced EMT and regulates the expression of FoxC1 and Snail

In determine if hsa_circ_0061052 is involved in the EMT, three siRNAs targeting hsa_circ_0061052 were designed to suppress its expression; their efficiency was tested (Fig. 4a). All three siRNAs down-regulated

hsa_circ_0061052 in HBE cells. Since hsa_circ_0061052 siRNA #1 was most effective, for further research, it was transfected into HBE cells.

Knockdown of hsa_circ_0061052 in HBE cells reduced the CSE-induced decrease in the levels of E-cadherin and the increase in levels of N-cadherin, vimentin, and α-SMA (Fig. 4b and c). Immunofluorescence microscopy showed that, after transfection of CSE-HBE cells with hsa_circ_0061052 siRNA, the level of E-cadherin increased, and the level of vimentin decreased (Fig. 4d). To determine if hsa_circ_0061052 was involved in the CSE-induced EMT through miR-515-5p/FoxC1 signaling, we determined whether hsa_circ_0061052 regulated the expression of FoxC1/Snail. In CSE-HBE cells transfected with hsa_circ_0061052 siRNA, the expressions of FoxC1 and Snail were lower compared with the control group (Fig. 4e and f). Thus, in the process of CSE-induced EMT in HBE cells, hsa_circ_0061052 regulates the expression of FoxC1 and Snail.

In HBE cells, miR-515-5p is involved in the CSE-induced EMT and regulates the expression of FoxC1 and Snail

We used bioinformatics tools to predict that FoxC1 is a target of miR-515-5p. To determine whether miR-515-5p reverses the CSE-induced EMT process, we transfected a miR-515-5p mimic into HBE cells (Fig. 5a). Western blots showed that ectopic expression of miR-515-5p attenuated the CSE-induced reduction of the levels of E-cadherin and the increased levels of N-cadherin, vimentin, and α-SMA (Fig. 5b and c). Immunofluorescence microscopy revealed that, after transfection of CSE-HBE cells with the miR-515-5p mimic, the levels of E-cadherin increased, and the levels of vimentin decreased (Fig. 5d). Compared with the CSE-HBE group, the levels of FoxC1 and Snail were lower in CSE-HBE cells transfected with miR-515-5p (Fig. 5e and f). These results show that, for HBE cells, miR-515-5p participates in the CSE-induced EMT and regulates the expression of FoxC1 and Snail.

In HBE cells, hsa_circ_0061052, via miR-515-5p regulation of FoxC1 and Snail, is involved in the CSE-induced EMT

Since hsa_circ_0061052 works in combination with miR-515-5p, rescue experiments were performed to determine if miR-515-5p is involved in the function of hsa_circ_0061052 in the CSE-induced EMT. Hsa_circ_0061052 siRNA or hsa_circ_0061052 siRNA and an miR-515-5p inhibitor were co-transfected into HBE cells. The qRT-PCR results showed that hsa_circ_0061052 siRNA did not affect the expression of miR-515-5p (Fig. 6a). However, the miR-515-5p inhibitor reversed the increase in E-cadherin caused by knockdown of hsa_circ_0061052 and the decreases in N-cadherin, vimentin, and α-SMA (Fig. 6b and c). Immunofluorescence microscopy showed that co-transfection of hsa_circ_0061052 siRNA and the miR-515-5p inhibitor reversed the effect of hsa_circ_0061052 siRNA in reducing the EMT (Fig. 6d). Further, knockdown of hsa_circ_0061052 reduced the levels of FoxC1 and Snail; this decrease was reversed by inhibition of miR-515-5p (Fig. 6e And f). Thus, these results show that, for HBE cells, hsa_circ_0061052 regulates FoxC1 and Snail by acting as a sponge for miR-515-5p and that it participates in the CSE-induced EMT.

Exposure of mice to CS increases the levels of hsa_circ_0061052 and decreases the levels of miR-515-5p in lung tissue, induces the EMT in lung tissue, and promotes airway obstruction

Mice are widely used to study the lung pathology in CS-induced COPD [1]. Mice were placed in a systemic exposure system, and the CS concentrations were set at 0, 100, 200, and 350 mg/m^3 total particulate matter (TPM) for the control group and the low, medium, and high CS exposure groups, respectively. After exposure of mice to CS, the levels of has_circ_0061052 increased in a dose-dependent manner; the levels of miR-515-5p decreased in a dose-dependent manner (Fig. 7a and b). For each group of mice dosed with 0, 12.5, 25, or 50 μg/mL methacholine, AHR (Penh value) was measured by whole body plethysmography as changes in mouse airway function [32]. As the concentration of methacholine increased, mice in each group showed enhanced AHR, and as the CS concentration increased, the Penh value showed an upward trend, indicating that the small airway resistance of the mice increased (Fig. 7c). With increasing exposure to CS, the levels of E-cadherin decreased, and those of N-cadherin, vimentin, and α-SMA increased (Fig. 7d and e). Masson trichrome staining showed that, as CS exposure increased, the small airways of mice thickened, and collagen was deposited. IHC assessment of mouse lung tissue showed an increase in collagen content and in the expression of α-SMA (Fig. 7f, g and h). These results show that, for mice, CS causes lung dysfunction and small airway remodeling. We conclude that hsa_circ_0061052 is involved in the effect of CS by inducing the EMT in airway epithelial cells through regulation of miR-515-5p, causing the airway remodeling associated with COPD (Fig. 8).

Discussion

Worldwide, there are 384 million COPD patients, and about 3 million people die each year from the disease. According to the World Health Organization, by 2030, COPD will be the third leading cause of death in the world (https://www.who.int/topics/chronic_obstructive_pulmonary_disease/en/). COPD covers a series of lung diseases whose anatomical features are small airway remodeling and emphysema [33]. Airway remodeling is characterized by epithelial damage, subepithelial fibrosis, smooth muscle hyperplasia and hypertrophy, goblet cell metaplasia, collagen deposition, and reticular basement membrane thickening [34]. Our previous studies show that CS induces airway remodeling, resulting in irreversible airflow restriction and increased airway hyperresponsiveness [8, 35]. In the present study, the small airway resistance of mice increased as CS exposure increased. Masson trichrome staining and IHC experiments demonstrated that, for mice, CS exposure causes small airway thickening and collagen deposition. Expression of the fibrosis marker, α-SMA, increased. Thus, for mice, CS causes lung dysfunction and small airway remodeling.

The EMT is associated with airway disease and fibrosis in multiple organs, including the lungs. Hallmarks of the EMT are loss of epithelial markers (such as E-cadherin) and increased interstitial phenotype (such as vimentin and α-SMA) [36]. CS induces the EMT in human bronchial epithelial cells [37], and the EMT in airway epithelial cells is a key event for COPD remodeling [38, 39]. The present study shows that lung tissue from CS-exposed mice and CSE-treated HBE cells have down-regulated epithelial

markers and up-regulated endothelial markers. Further, CSE induces the EMT, the transformation of epithelial cells to mesenchymal cells, and airway remodeling.

CircRNAs, non-coding RNAs that are widely expressed in eukaryotes [40], have a cyclic structure and are not readily degraded by RNase R [41]. CircRNAs are linked to the occurrence, development, and progression of lung diseases [21, 42, 43]. The present study is the first to explore the involvement of circRNAs in COPD. For HSAECs, a COPD cell model, CSE caused upregulation of hsa_circ_0061052 [22]. We focused on hsa_circ_0061052, derived from the host gene *OSBPL2*; it is 253 nucleotides in length and is resistant to degradation by RNase R. Its expression was up-regulated in CSE-treated HBE cells and in lung tissue of CS-exposed mice, suggesting that hsa_circ_0061052 is related to the occurrence of COPD. Sub-cellular localization is associated with the biological function of non-coding RNAs. CircRNAs in the cytoplasm can combine with miRNAs to perform functions of competing endogenous RNAs (ceRNAs) [44]. Hsa_circ_0061052 was mainly distributed in the cytoplasm. By use of bioinformatics methods, we predicted that hsa_circ_0061052 could bind to several miRNAs, and through screening, we found that hsa_circ_0061052 binds to miR-515-5p. Luciferase reporter experiments confirmed the interaction between hsa_circ_0061052 and miR-515-5p, indicating that hsa_circ_0061052 acts as a sponge for miR-515-5p. To evaluate, with HBE cells, the molecular mechanism of circRNA and its role in the EMT, hsa_circ_0061052 was silenced. The decrease of the epithelial marker protein, E-cadherin, caused by CSE was moderated, and levels of the mesenchymal markers, N-cadherin, vimentin, and α-SMA, were elevated.

The FOX protein functions as a typical transcription factor; other members of the family participate in regulation of chromatin remodeling and work with other transcription factors to regulate gene transcription [45]. Some members of the FOX family function in induction of the EMT [46]. For example, FOXD4 binds to the SNAIL3 promoter to support colorectal cancer metastasis [47], and FOXG1 mediates liver cancer metastasis through the Wnt/β-catenin pathway [48]. Snail, an E-cadherin transcription inhibitor, is a transcription target of FoxC1. In liver cancers, FoxC1 activates Snai1 expression by binding to the Snai1 promoter, thereby inhibiting the transcription of E-cadherin [25]. By targeting the 3'-UTR region of FOXC1 mRNA, miR-374c-5p inhibits expression of FOXC1, thereby inhibiting the function of Snail in regulating the EMT of cervical cancer cells [49].

In the present study, we used bioinformatics tools to predict that miR-515-5p acts on the 3'-UTR region of FoxC1 mRNA. The results of luciferase reporter experiments showed that FoxC1 mRNA is a target of miR-515-5p and that, in HBE cells, CSE increased the levels of FoxC1 and Snail. Results of experiments with mice were consistent with these findings. After transfection of cells with an miR-515-5p mimic, the ectopic expression of miR-515-5p attenuated the CSE-induced EMT process and reduced the expression levels of FoxC1 and Snail, indicating that miR-515-5p and FoxC1/Snail participate in the EMT of HBE cells. CircRNAs, long non-coding RNAs, and various other RNA transcripts, including those of pseudogenes, can function as ceRNAs and participate in the development of human diseases [50]. The present results indicate that hsa_circ_0061052 is a ceRNA for miR-515-5p to down-regulate the expression of its target gene, *FoxC1*. Knockdown of hsa_circ_0061052 reduced the CSE-induced EMT, an effect that was reversed by transfection with an inhibitor of miR-515-5p.

Conclusion

In conclusion, our findings show that, by regulating miR-515-5p through a FoxC1/Snail regulatory axis, hsa_circ_0061052 is involved in the airway remodeling of COPD caused by CS and indicate that hsa_circ_0000515 is a target for therapy of COPD.

Abbreviations

ncRNA: non-coding RNA; circRNA: circular RNA; COPD: chronic obstructive pulmonary disease; CSE: cigarette smoke extract; CS: cigarette smoke; EMT: epithelial-mesenchymal transition; Fox: forkhead box; ceRNAs: competing endogenous RNAs; FISH: Fluorescence in situ hybridization assay; AHR: airway hyper-responsiveness; OSBPL2: oxysterol-binding protein 2; TPM: total particulate matter; IHC: Immunohistochemistry;

Declarations

Acknowledgments

The authors wish to thank Donald L. Hill (University of Alabama at Birmingham, USA), an experienced, English-speaking scientific editor, for editing.

Authors' contributions

Huimin Ma, Lu Lu, Haibo Xia performed the majority of the experiments. Huimin Ma and Lu Lu analyzed the data and wrote the manuscript. Jing Sun, Junchao Xue, Tian Xiao and Cheng Cheng performed the in vivo experiments. Qizhan Liu Aimin Shi and Quanyong Xiang conceived idea, chiefly carried out data analysis and interpretation. All authors read and approved the final manuscript.

Funding

This work was supported by the Natural Science Foundations of China (81803276, 81973085, 81973005) and the Priority Academic Program Development of Jiangsu Higher Education Institutions (2019).

Availability of data and materials

The datasets supporting the conclusions of this article are included within

the article and its additional files.

Ethics approval and consent to participate

No ethics approval was required for this study that did not involve patients

or patient data.

Consent for publication

All authors consent to publication.

Competing interests

The authors declare that they have no competing interests.

References

1. Polverino F, Doyle-Eisele M, McDonald J, Wilder JA, Royer C, Laucho-Contreras M, Kelly EM, Divo M, Pinto-Plata V, Mauderly J, et al: **A novel nonhuman primate model of cigarette smoke-induced airway disease.** *Am J Pathol* 2015, **185:**741-755.
2. Vij N, Chandramani-Shivalingappa P, Van Westphal C, Hole R, Bodas M: **Cigarette smoke-induced autophagy impairment accelerates lung aging, COPD-emphysema exacerbations and pathogenesis.** *Am J Physiol Cell Physiol* 2018, **314:**C73-C87.
3. Hou W, Hu S, Li C, Ma H, Wang Q, Meng G, Guo T, Zhang J: **Cigarette Smoke Induced Lung Barrier Dysfunction, EMT, and Tissue Remodeling: A Possible Link between COPD and Lung Cancer.** *Biomed Res Int* 2019, **2019:**2025636.
4. McDonough JE, Yuan R, Suzuki M, Seyednejad N, Elliott WM, Sanchez PG, Wright AC, Gefter WB, Litzky L, Coxson HO, et al: **Small-airway obstruction and emphysema in chronic obstructive pulmonary disease.** *N Engl J Med* 2011, **365:**1567-1575.
5. Gohy ST, Hupin C, Fregimilicka C, Detry BR, Bouzin C, Gaide Chevronay H, Lecocq M, Weynand B, Ladjemi MZ, Pierreux CE, et al: **Imprinting of the COPD airway epithelium for dedifferentiation and mesenchymal transition.** *Eur Respir J* 2015, **45:**1258-1272.
6. Eapen MS, Sharma P, Gaikwad AV, Lu W, Myers S, Hansbro PM, Sohal SS: **Epithelial-mesenchymal transition is driven by transcriptional and post transcriptional modulations in COPD: implications for disease progression and new therapeutics.** *Int J Chron Obstruct Pulmon Dis* 2019, **14:**1603-1610.
7. Lin L, Hou G, Han D, Yin Y, Kang J, Wang Q: **Ursolic acid alleviates airway-vessel remodeling and muscle consumption in cigarette smoke-induced emphysema rats.** *BMC Pulm Med* 2019, **19:**103.
8. Xia H, Xue J, Xu H, Lin M, Shi M, Sun Q, Xiao T, Dai X, Wu L, Li J, et al: **Andrographolide antagonizes the cigarette smoke-induced epithelial-mesenchymal transition and pulmonary dysfunction through anti-inflammatory inhibiting HOTAIR.** *Toxicology* 2019, **422:**84-94.
9. Dasgupta P, Rizwani W, Pillai S, Kinkade R, Kovacs M, Rastogi S, Banerjee S, Carless M, Kim E, Coppola D, et al: **Nicotine induces cell proliferation, invasion and epithelial-mesenchymal transition in a variety of human cancer cell lines.** *Int J Cancer* 2009, **124:**36-45.
10. Zhao Y, Xu Y, Li Y, Xu W, Luo F, Wang B, Pang Y, Xiang Q, Zhou J, Wang X, Liu Q: **NF-kappaB-mediated inflammation leading to EMT via miR-200c is involved in cell transformation induced by cigarette smoke extract.** *Toxicol Sci* 2013, **135:**265-276.

11. Liu Y, Luo F, Xu Y, Wang B, Zhao Y, Xu W, Shi L, Lu X, Liu Q: **Epithelial-mesenchymal transition and cancer stem cells, mediated by a long non-coding RNA, HOTAIR, are involved in cell malignant transformation induced by cigarette smoke extract.** *Toxicol Appl Pharmacol* 2015, **282:**9-19.
12. Horvat N, Locatelli I, Kos M, Janezic A: **Medication adherence and health-related quality of life among patients with chronic obstructive pulmonary disease.** *Acta Pharm* 2018, **68:**117-125.
13. Pandey PR, Rout PK, Das A, Gorospe M, Panda AC: **RPAD (RNase R treatment, polyadenylation, and poly(A)+ RNA depletion) method to isolate highly pure circular RNA.** *Methods* 2019, **155:**41-48.
14. Bolha L, Ravnik-Glavac M, Glavac D: **Circular RNAs: Biogenesis, Function, and a Role as Possible Cancer Biomarkers.** *Int J Genomics* 2017, **2017:**6218353.
15. Memczak S, Jens M, Elefsinioti A, Torti F, Krueger J, Rybak A, Maier L, Mackowiak SD, Gregersen LH, Munschauer M, et al: **Circular RNAs are a large class of animal RNAs with regulatory potency.** *Nature* 2013, **495:**333-338.
16. Cheng X, Zhang L, Zhang K, Zhang G, Hu Y, Sun X, Zhao C, Li H, Li YM, Zhao J: **Circular RNA VMA21 protects against intervertebral disc degeneration through targeting miR-200c and X linked inhibitor-of-apoptosis protein.** *Ann Rheum Dis* 2018, **77:**770-779.
17. Zeng X, Zhong Y, Lin W, Zou Q: **Predicting disease-associated circular RNAs using deep forests combined with positive-unlabeled learning methods.** *Brief Bioinform* 2019.
18. Zhao R, Ni J, Lu S, Jiang S, You L, Liu H, Shou J, Zhai C, Zhang W, Shao S, et al: **CircUBAP2-mediated competing endogenous RNA network modulates tumorigenesis in pancreatic adenocarcinoma.** *Aging (Albany NY)* 2019, **11:**8484-8501.
19. Chen X, Mao R, Su W, Yang X, Geng Q, Guo C, Wang Z, Wang J, Kresty LA, Beer DG, et al: **Circular RNA circHIPK3 modulates autophagy via MIR124-3p-STAT3-PRKAA/AMPKalpha signaling in STK11 mutant lung cancer.** *Autophagy* 2019**:**1-13.
20. Nan A, Chen L, Zhang N, Jia Y, Li X, Zhou H, Ling Y, Wang Z, Yang C, Liu S, Jiang Y: **Circular RNA circNOL10 Inhibits Lung Cancer Development by Promoting SCLM1-Mediated Transcriptional Regulation of the Humanin Polypeptide Family.** *Adv Sci (Weinh)* 2019, **6:**1800654.
21. Huang Z, Cao Y, Zhou M, Qi X, Fu B, Mou Y, Wu G, Xie J, Zhao J, Xiong W: **Hsa_circ_0005519 increases IL-13/IL-6 by regulating hsa-let-7a-5p in CD4(+) T cells to affect asthma.** *Clin Exp Allergy* 2019, **49:**1116-1127.
22. Zeng N, Wang T, Chen M, Yuan Z, Qin J, Wu Y, Gao L, Shen Y, Chen L, Wen F: **Cigarette smoke extract alters genome-wide profiles of circular RNAs and mRNAs in primary human small airway epithelial cells.** *J Cell Mol Med* 2019, **23:**5532-5541.
23. Zhu X, Wei L, Bai Y, Wu S, Han S: **FoxC1 promotes epithelial-mesenchymal transition through PBX1 dependent transactivation of ZEB2 in esophageal cancer.** *Am J Cancer Res* 2017, **7:**1642-1653.
24. Huang L, Huang Z, Fan Y, He L, Ye M, Shi K, Ji B, Huang J, Wang Y, Li Q: **FOXC1 promotes proliferation and epithelial-mesenchymal transition in cervical carcinoma through the PI3K-AKT signal pathway.** *Am J Transl Res* 2017, **9:**1297-1306.

25. Xia L, Huang W, Tian D, Zhu H, Qi X, Chen Z, Zhang Y, Hu H, Fan D, Nie Y, Wu K: **Overexpression of forkhead box C1 promotes tumor metastasis and indicates poor prognosis in hepatocellular carcinoma.** *Hepatology* 2013, **57:**610-624.
26. Jobse BN, Rhem RG, Wang IQ, Counter WB, Stampfli MR, Labiris NR: **Detection of lung dysfunction using ventilation and perfusion SPECT in a mouse model of chronic cigarette smoke exposure.** *J Nucl Med* 2013, **54:**616-623.
27. Livak KJ, Schmittgen TD: **Analysis of relative gene expression data using real-time quantitative PCR and the 2(-Delta Delta C(T)) Method.** *Methods* 2001, **25:**402-408.
28. Wang Y, Jia M, Yan X, Cao L, Barnes PJ, Adcock IM, Huang M, Yao X: **Increased neutrophil gelatinase-associated lipocalin (NGAL) promotes airway remodelling in chronic obstructive pulmonary disease.** *Clin Sci (Lond)* 2017, **131:**1147-1159.
29. Marudamuthu AS, Bhandary YP, Shetty SK, Fu J, Sathish V, Prakash Y, Shetty S: **Role of the urokinase-fibrinolytic system in epithelial-mesenchymal transition during lung injury.** *Am J Pathol* 2015, **185:**55-68.
30. Wang G, Guo X, Cheng L, Chu P, Chen M, Chen Y, Chang C: **An integrated analysis of the circRNA-miRNA-mRNA network reveals novel insights into potential mechanisms of cell proliferation during liver regeneration.** *Artif Cells Nanomed Biotechnol* 2019, **47:**3873-3884.
31. Guan YJ, Ma JY, Song W: **Identification of circRNA-miRNA-mRNA regulatory network in gastric cancer by analysis of microarray data.** *Cancer Cell Int* 2019, **19:**183.
32. Rajavelu P, Chen G, Xu Y, Kitzmiller JA, Korfhagen TR, Whitsett JA: **Airway epithelial SPDEF integrates goblet cell differentiation and pulmonary Th2 inflammation.** *J Clin Invest* 2015, **125:**2021-2031.
33. Tam A, Churg A, Wright JL, Zhou S, Kirby M, Coxson HO, Lam S, Man SF, Sin DD: **Sex Differences in Airway Remodeling in a Mouse Model of Chronic Obstructive Pulmonary Disease.** *Am J Respir Crit Care Med* 2016, **193:**825-834.
34. Nie L, Liu ZJ, Zhou WX, Xiang RL, Xiao Y, Lu B, Pang BS, Gao JM: **Chemokine receptor CXCR3 is important for lung tissue damage and airway remodeling induced by short-term exposure to cigarette smoking in mice.** *Acta Pharmacol Sin* 2010, **31:**436-442.
35. Xu H, Ling M, Xue J, Dai X, Sun Q, Chen C, Liu Y, Zhou L, Liu J, Luo F, et al: **Exosomal microRNA-21 derived from bronchial epithelial cells is involved in aberrant epithelium-fibroblast cross-talk in COPD induced by cigarette smoking.** *Theranostics* 2018, **8:**5419-5433.
36. Nowrin K, Sohal SS, Peterson G, Patel R, Walters EH: **Epithelial-mesenchymal transition as a fundamental underlying pathogenic process in COPD airways: fibrosis, remodeling and cancer.** *Expert Rev Respir Med* 2014, **8:**547-559.
37. Zou W, Zou Y, Zhao Z, Li B, Ran P: **Nicotine-induced epithelial-mesenchymal transition via Wnt/beta-catenin signaling in human airway epithelial cells.** *Am J Physiol Lung Cell Mol Physiol* 2013, **304:**L199-209.
38. Jeffery PK: **Remodeling and inflammation of bronchi in asthma and chronic obstructive pulmonary disease.** *Proc Am Thorac Soc* 2004, **1:**176-183.

39. Sohal SS, Reid D, Soltani A, Ward C, Weston S, Muller HK, Wood-Baker R, Walters EH: **Reticular basement membrane fragmentation and potential epithelial mesenchymal transition is exaggerated in the airways of smokers with chronic obstructive pulmonary disease.** *Respirology* 2010, **15:**930-938.
40. Li X, Yang L, Chen LL: **The Biogenesis, Functions, and Challenges of Circular RNAs.** *Mol Cell* 2018, **71:**428-442.
41. Chen LL, Yang L: **Regulation of circRNA biogenesis.** *RNA Biol* 2015, **12:**381-388.
42. Qu D, Yan B, Xin R, Ma T: **A novel circular RNA hsa_circ_0020123 exerts oncogenic properties through suppression of miR-144 in non-small cell lung cancer.** *Am J Cancer Res* 2018, **8:**1387-1402.
43. Yang P, Gao R, Zhou W, Han A: **Protective impacts of circular RNA VMA21 on lipopolysaccharide-engendered WI-38 cells injury via mediating microRNA-142-3p.** *Biofactors* 2019.
44. Sulaiman SA, Abdul Murad NA, Mohamad Hanif EA, Abu N, Jamal R: **Prospective Advances in Circular RNA Investigation.** *Adv Exp Med Biol* 2018, **1087:**357-370.
45. Katoh M, Igarashi M, Fukuda H, Nakagama H, Katoh M: **Cancer genetics and genomics of human FOX family genes.** *Cancer Lett* 2013, **328:**198-206.
46. Cai J, Tian AX, Wang QS, Kong PZ, Du X, Li XQ, Feng YM: **FOXF2 suppresses the FOXC2-mediated epithelial-mesenchymal transition and multidrug resistance of basal-like breast cancer.** *Cancer Lett* 2015, **367:**129-137.
47. Chen C, Aihemaiti M, Zhang X, Qu H, Jiao J, Sun Q, Yu W: **FOXD4 induces tumor progression in colorectal cancer by regulation of the SNAI3/CDH1 axis.** *Cancer Biol Ther* 2018, **19:**1065-1071.
48. Zheng X, Lin J, Wu H, Mo Z, Lian Y, Wang P, Hu Z, Gao Z, Peng L, Xie C: **Forkhead box (FOX) G1 promotes hepatocellular carcinoma epithelial-Mesenchymal transition by activating Wnt signal through forming T-cell factor-4/Beta-catenin/FOXG1 complex.** *J Exp Clin Cancer Res* 2019, **38:**475.
49. Huang Y, Huang H, Li M, Zhang X, Liu Y, Wang Y: **MicroRNA-374c-5p regulates the invasion and migration of cervical cancer by acting on the Foxc1/snail pathway.** *Biomed Pharmacother* 2017, **94:**1038-1047.
50. Tay Y, Rinn J, Pandolfi PP: **The multilayered complexity of ceRNA crosstalk and competition.** *Nature* 2014, **505:**344-352.

Figures

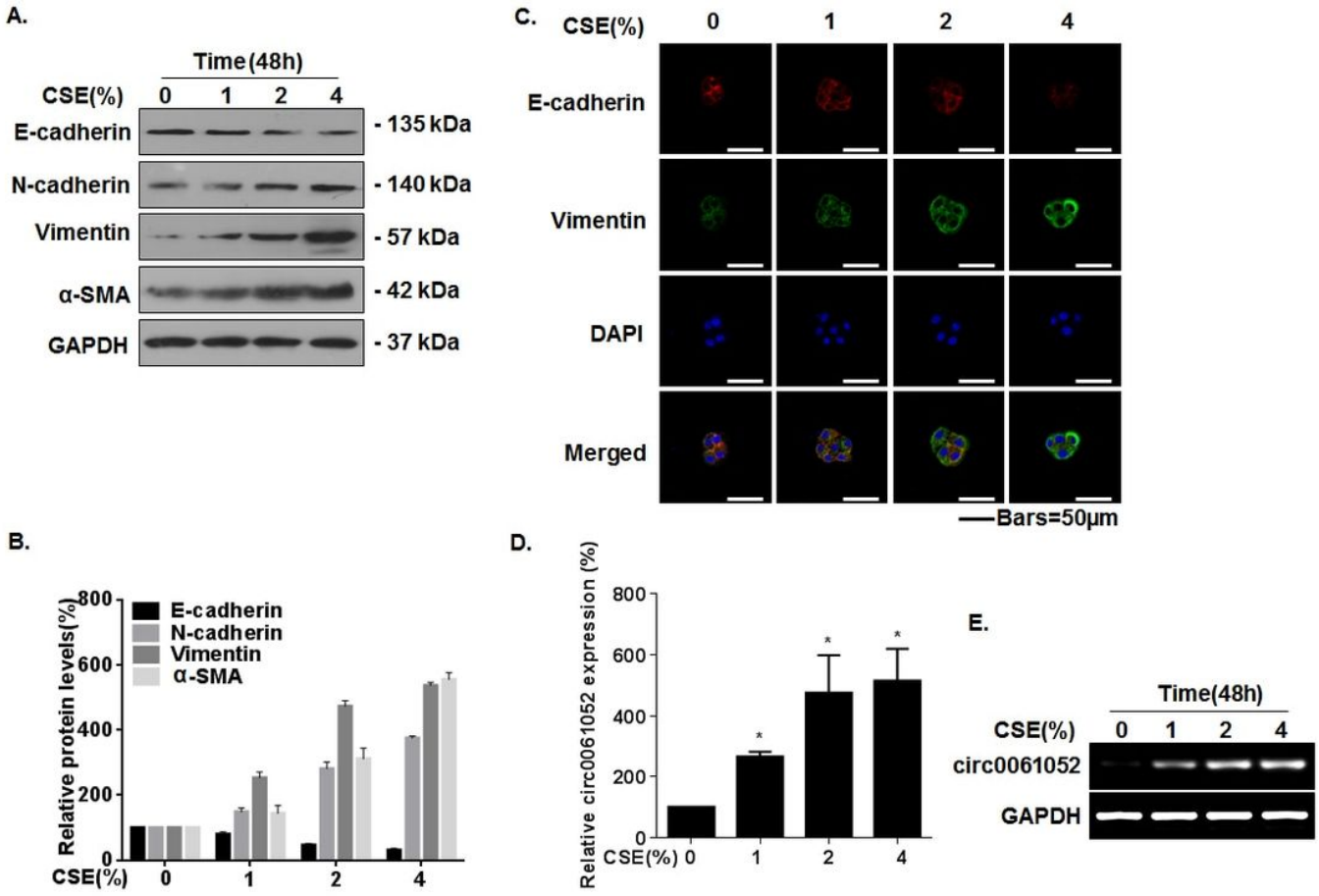

Figure 1

CSE exposure induces the EMT and increases the levels of hsa_circ_0061052 in HBE cells. Band density was quantified by Image J software. GAPDH levels, measured in parallel, served as controls. HBE cells were treated with 0, 1, 2, or 4% CSE for 48 hours. a Western blots were performed, and b relative protein levels of E-cadherin, N-cadherin, vimentin, and α-SMA were determined. c Immunofluorescence staining of E-cadherin and vimentin in HBE cells for the indicated groups. Red represents E-cadherin staining; green represents vimentin staining; and blue represents nuclear DNA staining by DAPI, bars = 50 μm. The levels of hsa_circ_0061052 in HBE cells were determined by quantitative RT-PCR d and by RT–PCR e. *$P < 0.05$, different from HBE cells without CSE. All data are presented as means ± SD for experiments conducted in triplicate.

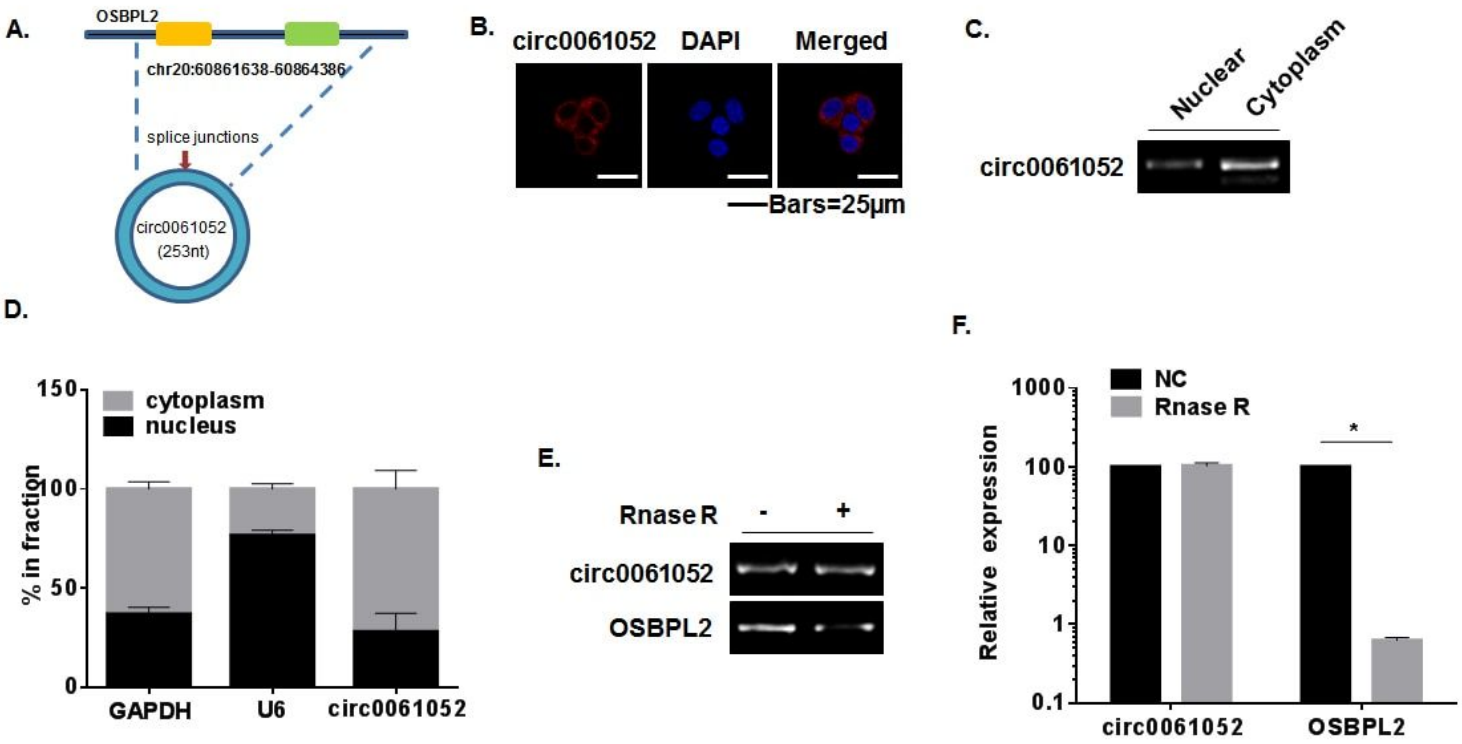

Figure 2

Characterization of hsa_circ_0061052 in HBE cells. GAPDH levels, measured in parallel, served as controls. a A schematic diagram of the origin of hsa_circ_0061052. b Determined by FISH, confocal microscope image showing that hsa_circ_0061052 is located in the cytoplasm. Red represents hsa_circ_0061052 staining, and blue represents DAPI staining of nuclear DNA; bars = 25 μM. The relative expression of hsa_circ_0061052 in the cytoplasm and nuclei of HBE cells was determined by RT-PCR c and quantitative RT-PCR d. The RNA levels of hsa_circ_0061052 and OSBPL2 in HBE cells were determined by RT-PCR e and quantitative RT-PCR f after 1 hour of total RNA treatment with or without 10 U RNase R, *P < 0.05, different from HBE cells without RNase R. All data are presented as means ± SD for experiments conducted in triplicate.

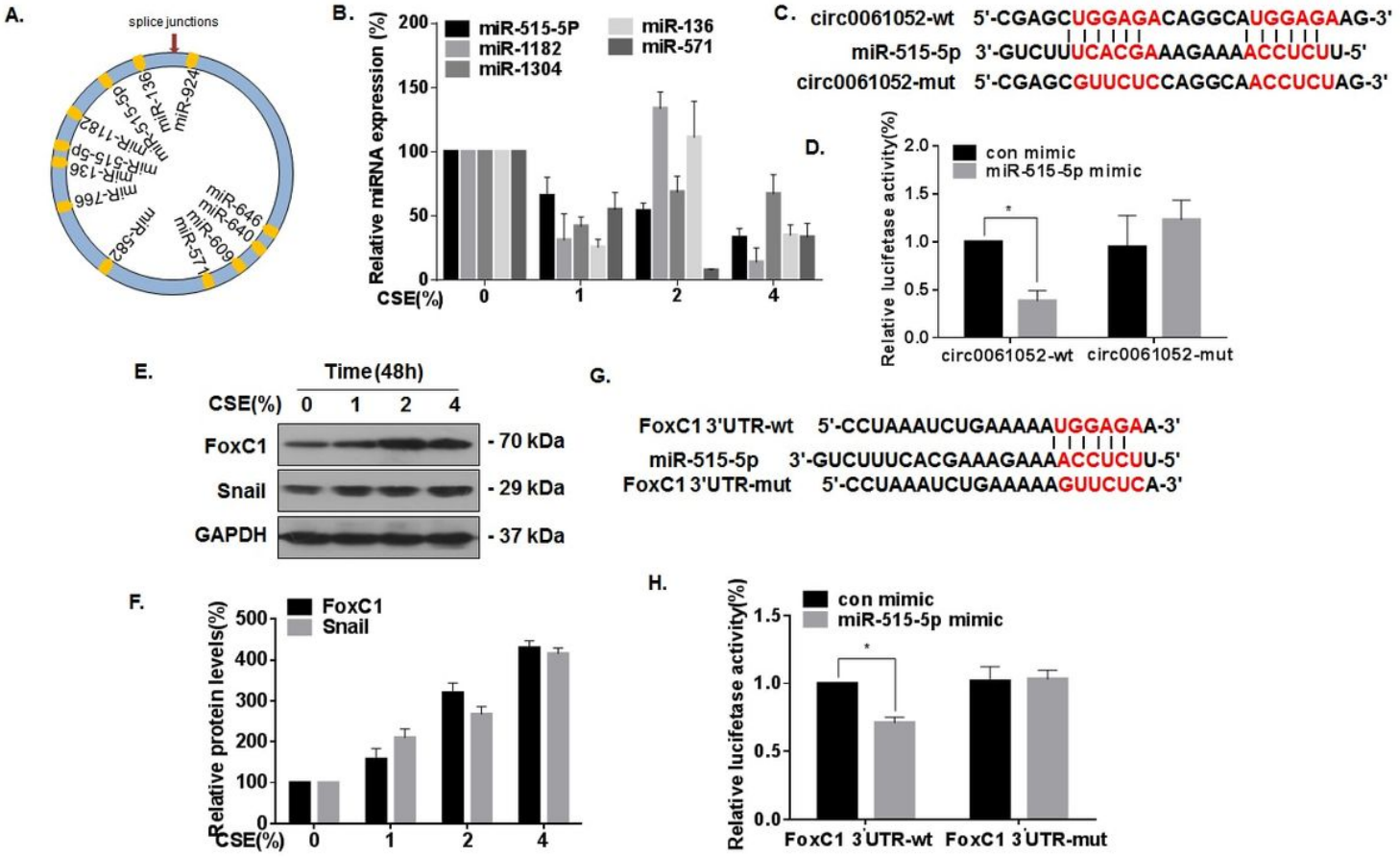

Figure 3

Exposure of HBE cells to CSE decreases their levels of miR-515-5p and increases their levels of FoxC1/Snail, which is a target of miR-515-5p. Band density was quantified by Image J software. GAPDH, measured in parallel, served as a control. a Schematic model showing the putative binding sites for miRNAs on hsa_circ_0061052. HBE cells were treated with 0, 1, 2, or 4% CSE for 48 hours. b The levels of miR-515-5p, miR-1182, miR-1304, miR-136, and miR-571 were determined by quantitative RT-PCR. c The predicted complementary binding sites within hsa_circ_0061052 and miR-515-5p. HBE cells were transfected with psiCHECK2-hsa_circ_0061052-wt or psiCHECK2-hsa_circ_0061052-mut for 24 hours, then transfected with an miR-515-5p mimic (50 nM). d Luciferase activity was measured at 48 hours after transfection, *P < 0.05, different from HBE cells co-transfected with a con mimic. HBE cells were treated with 0, 1, 2, or 4% CSE for 48 hours. e Western blots were performed, and f relative protein levels of FoxC1 and Snail were determined. g Schematic graph illustrating the binding sites of miR-515-5p in the 3'-UTR region of FoxC1 mRNA. HBE cells were transfected with psiCHECK2-FoxC1 3'-UTR-wt or psiCHECK2-FoxC1 3'-UTR-mut for 24 hours, then transfected with an miR-515-5p mimic (50 nM). h Luciferase activity was measured at 48 hours after transfection, *P < 0.05, different from HBE cells co-transfected with a con mimic. All data are presented as means ± SD for experiments conducted in triplicate.

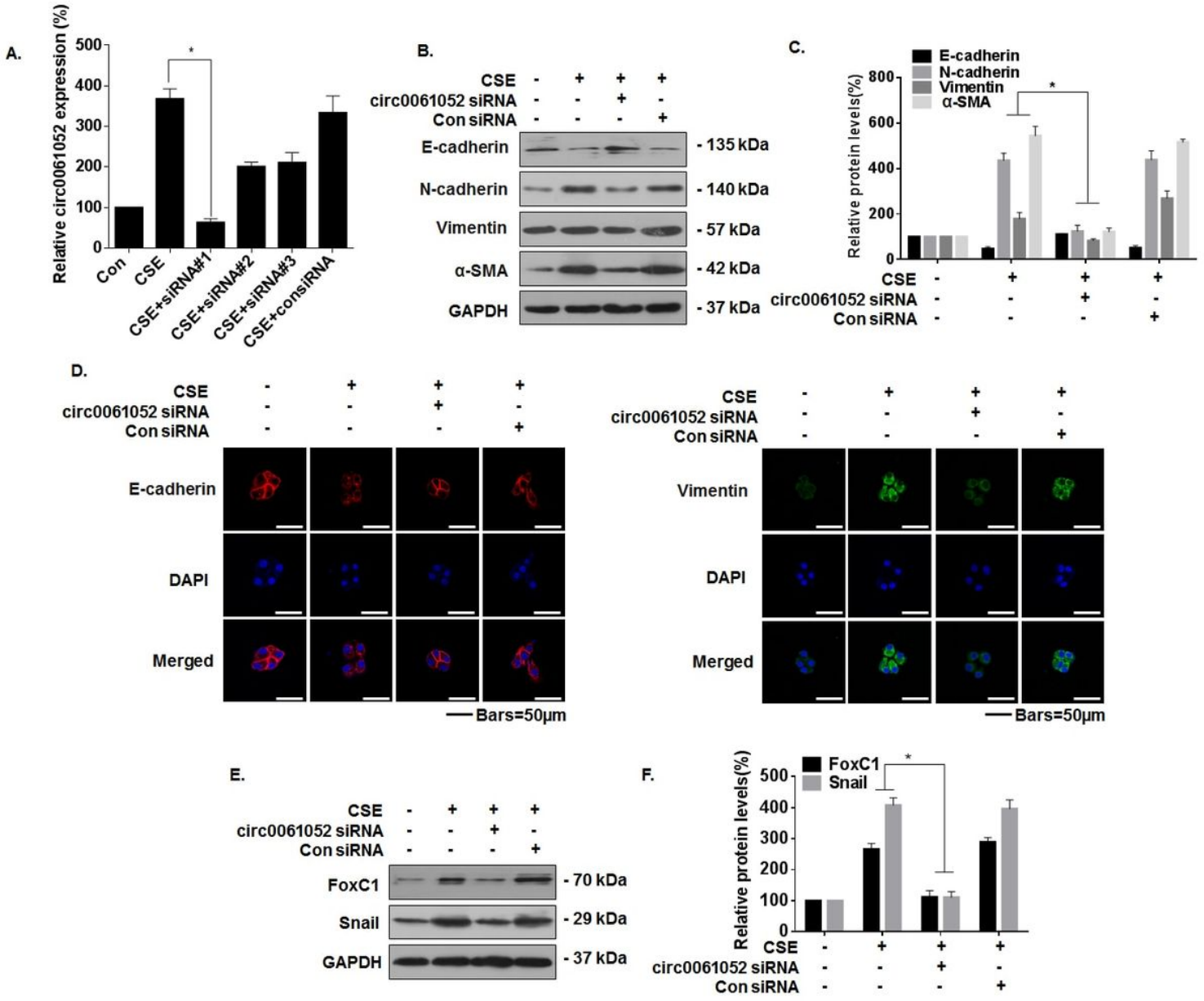

Figure 4

In HBE cells, hsa_circ_0061052 is involved in the CSE-induced EMT and regulates the expression of FoxC1 and Snail. Band density was quantified by Image J software. GAPDH, measured in parallel, served as a control. HBE cells were exposed to control siRNA or to one of three hsa_circ_0061052 siRNAs for 24 hours, then incubated with 2% CSE for 48 hours. a The relative mRNA levels of hsa_circ_0061052 were determined by quantitative RT-PCR. *P< 0.05, different from CSE-HBE cells in the absence of hsa_circ_0061052 siRNA #1. HBE cells were cultured in the presence of hsa_circ_0061052 siRNA (50 nM) or control siRNA for 24 hours, then exposed to 2% CSE for 48 hours. b Western blots were performed, and c relative protein levels of E-cadherin, N-cadherin, vimentin, and α-SMA were determined, *P< 0.05, different from CSE-HBE cells in the absence of hsa_circ_0061052 siRNA. d Immunofluorescence staining of E-cadherin and vimentin in HBE cells for the indicated groups. Green represents vimentin staining; red represents E-cadherin staining; and blue represents nuclear DNA staining by DAPI, bars = 50 μm. e

Western blots were performed, and f relative protein levels of FoxC1 and Snail were determined, *P< 0.05, different from CSE-HBE cells in the absence of hsa_circ_0061052 siRNA. All data are presented as means ± SD for experiments conducted in triplicate.

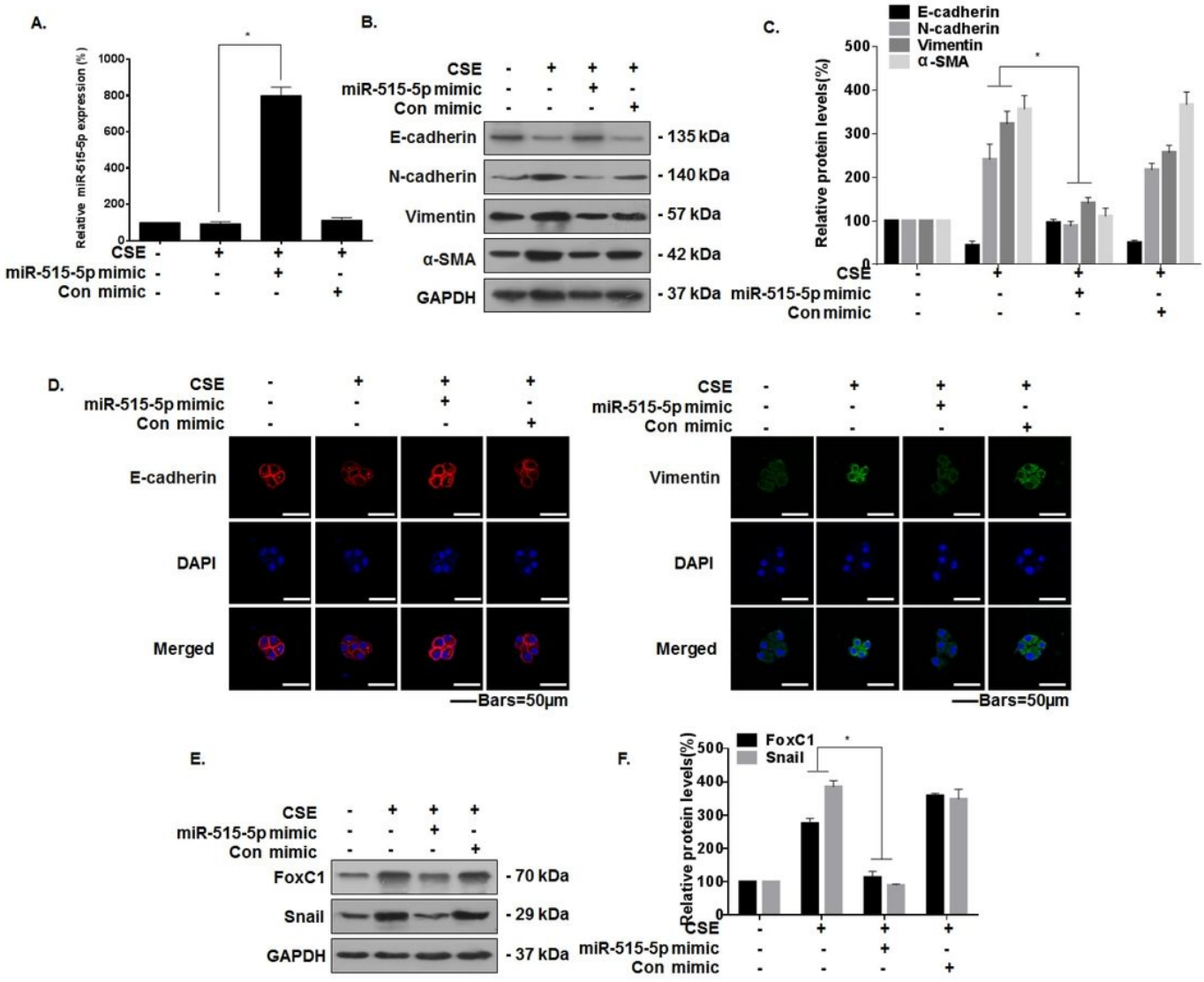

Figure 5

In HBE cells, miR-515-5p is involved in the CSE-induced EMT and regulates the expression of FoxC1 and Snail. Band density was quantified by Image J software. GAPDH, measured in parallel, served as a control. HBE cells were cultured in the presence of an miR-515-5p mimic (50 nM) or con mimic for 24 hours, then exposed to 2% CSE for 48 hours. a The miR-515-5p levels were determined by quantitative RT-PCR, *P< 0.05, different from CSE-HBE cells in the absence of the miR-515-5p mimic. b Western blots were performed, and c relative protein levels of E-cadherin, N-cadherin, vimentin, and α-SMA were determined, *P< 0.05, different from CSE-HBE cells in the absence of the miR-515-5p mimic. d Immunofluorescence staining of E-cadherin and vimentin in HBE cells for the indicated groups. Green represents vimentin staining; red represents E-cadherin staining; and blue represents nuclear DNA staining by DAPI, bars = 50 μm. e Western blots were performed, and f relative protein levels of FoxC1 and Snail

were determined. *P< 0.05, different from CSE-HBE cells in the absence of the miR-515-5p mimic. All data are presented as means ± SD for experiments conducted in triplicate.

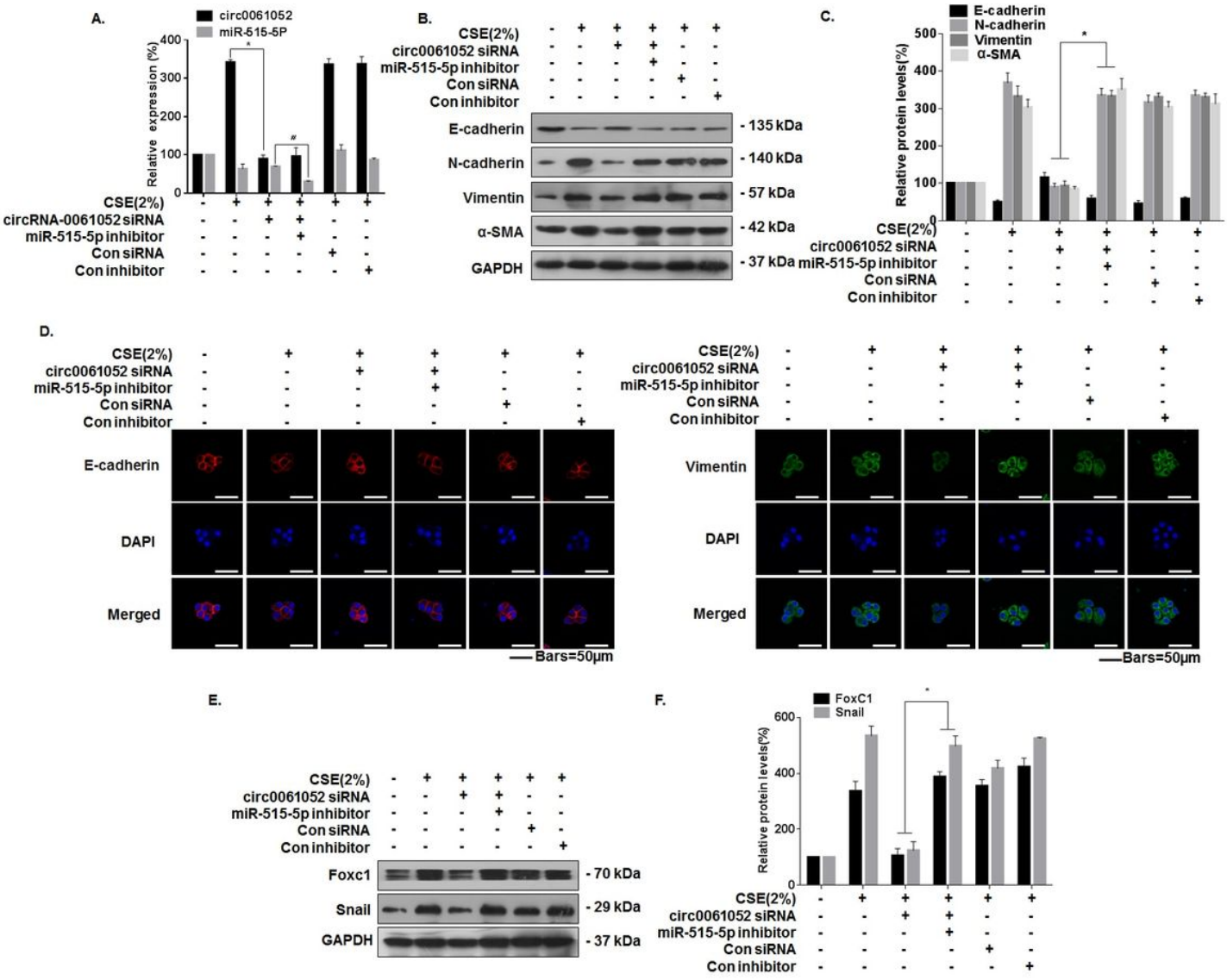

Figure 6

In HBE cells, hsa_circ_0061052, via miR-515-5p regulation of FoxC1 and Snail, is involved in the CSE-induced EMT. Band density was quantified by Image J software. GAPDH, measured in parallel, served as a control. HBE cells were co-transfected with hsa_circ_0061052 siRNA or with hsa_circ_0061052 siRNA + the miR-515-5p inhibitor for 24 hours, then exposed to 2% CSE for 48 hours. a The relative levels of hsa_circ_0061052 and miR-515-5p were determined by quantitative RT-PCR, *P< 0.05, different from CSE-HBE cells in the absence of hsa_circ_0061052 siRNA; #P< 0.05, different from CSE-HBE cells in the absence of the miR-515-5p inhibitor. b Western blots were performed, and c relative protein levels of E-cadherin, N-cadherin, vimentin, and α-SMA were determined. *P< 0.05, different from CSE-HBE cells in the absence of the miR-515-5p inhibitor. d Immunofluorescence staining of E-cadherin and vimentin in HBE cells for the indicated groups. Green represents vimentin staining; red represents E-cadherin staining; and blue represents nuclear DNA staining by DAPI, bars = 50 μm. e Western blots were performed, and f

relative protein levels of FoxC1 and Snail were determined, *P< 0.05, different from CSE-HBE cells in the absence of the miR-515-5p inhibitor. All data are presented as means ± SD for experiments conducted in triplicate.

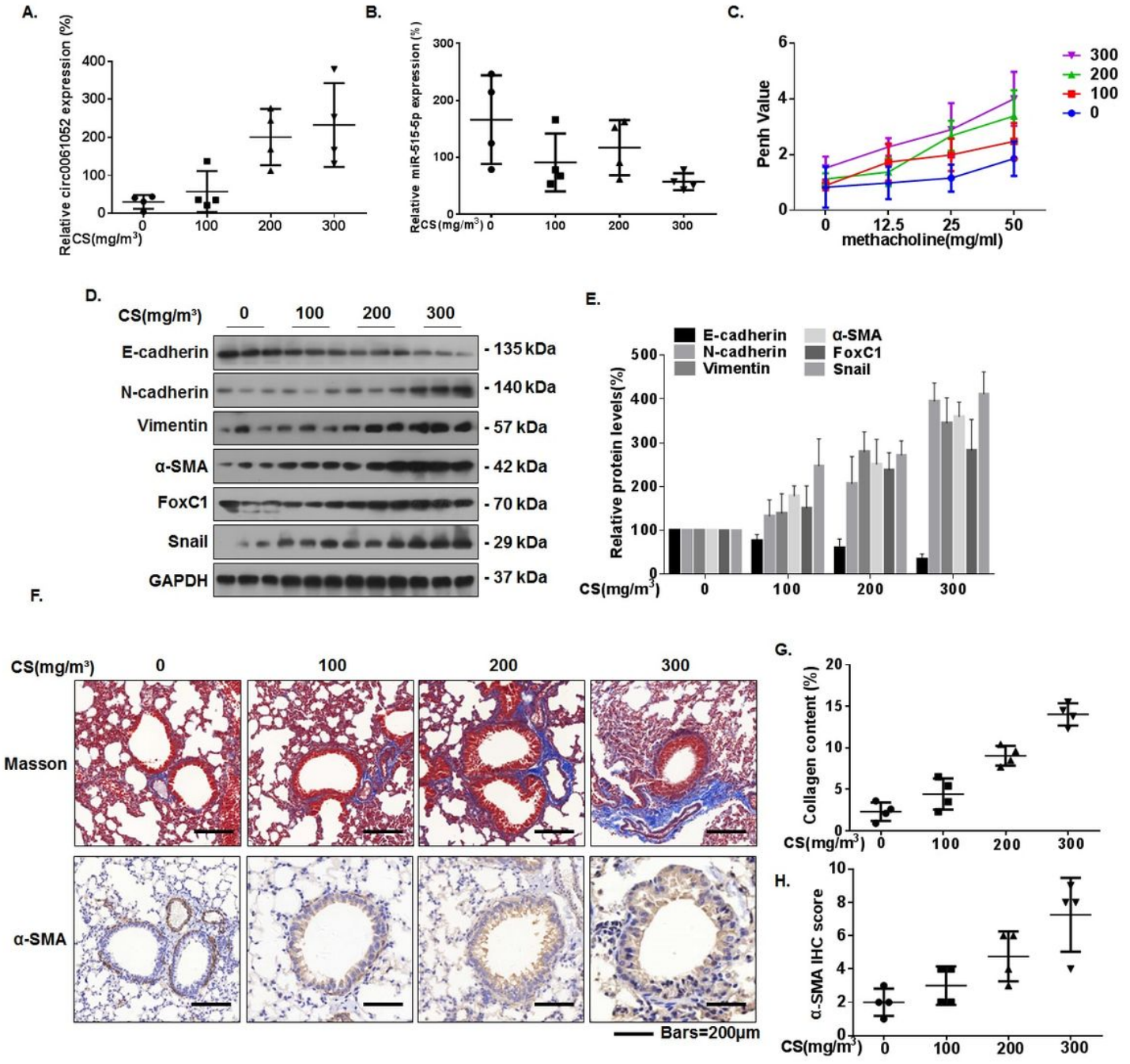

Figure 7

Exposure of mice to CS increases the levels of hsa_circ_0061052 and decreases the levels of miR-515-5p in lung tissue, induces the EMT in lung tissue, and promotes airway obstruction. Male BALB/c mice at 6-8 weeks of age were exposed to 0, 100, 200, or 300 mg/m3 TPM CS for 16 weeks. n=4 randomized animals per group. The levels of hsa_circ_0061052 in lung tissue a and the levels of miR-515-5p in lung tissue b were determined by quantitative RT-PCR. AHR is represented as Penh in normal control mice and CS-exposed mice in response to 0, 12.5, 25, or 50 μg/mL of methacholine. c Penh values were measured by

use of whole-body plethysmography. Densities of bands were quantified by Image J software. GAPDH, measured in parallel, served as a control. d Western blots were performed, and e relative protein levels of EMT-related markers (E-cadherin, N-cadherin, vimentin, and α-SMA), FoxC1, and Snail in lung tissue of mice were determined. f Representative images of lung sections after Masson trichrome staining and α-SMA IHC, bars = 200 μm. g Quantification of collagen content by Masson trichrome staining. h The levels of α-SMA as determined by IHC analyses. All data are presented as means ± SD for experiments conducted in triplicate.

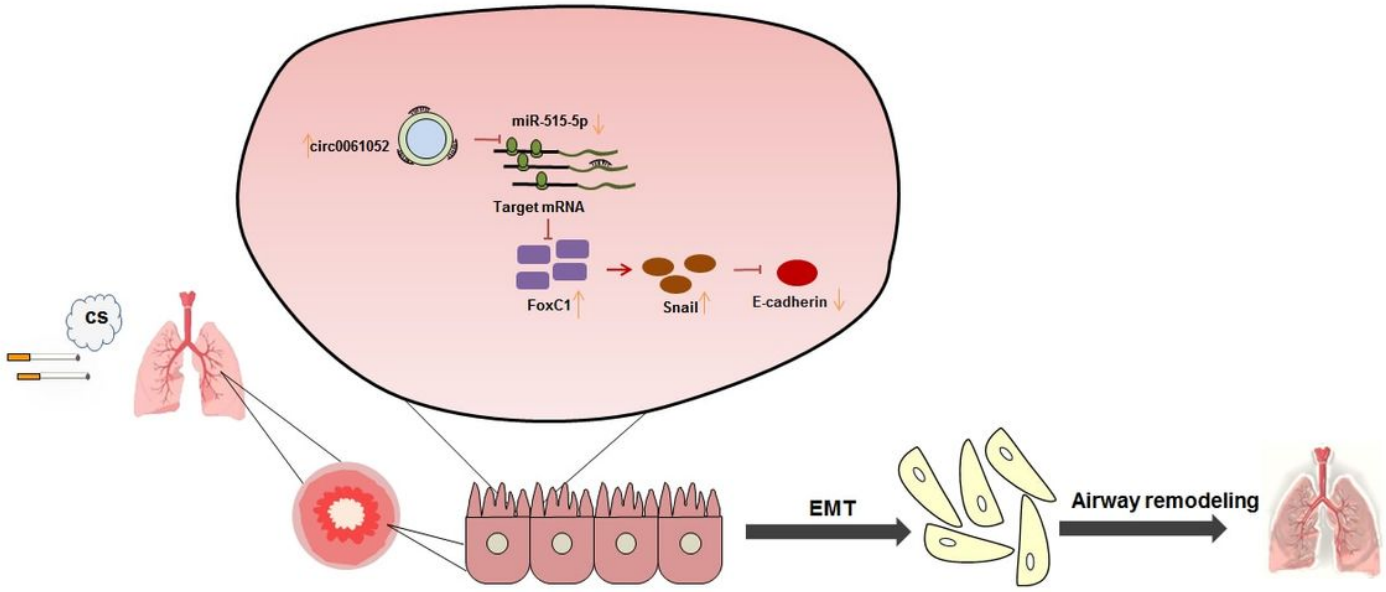

Figure 8

schematic diagram showing that circRNA-0061052 induces the EMT in airway epithelial cells exposed to CS by regulating miR-515-5p, causing COPD airway remodeling. Exposure of bronchial epithelial cells to CS increases their hsa_circ_0061052 levels. Hsa_circ_0061052 up-regulates the expression of the miR-515-5p target gene, FoxC1, by binding to miR-515-5p. FoxC1 activates Snail expression by binding to its promoter region, then inhibits the transcription of E-cadherin, increases the expression of mesenchymal marker proteins, induces the occurrence of EMT in HBE cells, and participates in airway remodeling, leading to COPD.